JMBFS

Journal of Microbiology, Biotechnology and Food Sciences

International peer-reviewed scientific online journal

Published by Faculty of Biotechnology and Food Sciences

ELUCIDATION OF ANTI-INFLAMMATORY ACTIVITY OF A NEW CYCLIC ALKALOID COMPOUND FROM ROOT BARK OF *ZIZIPHUS NUMMULARIA* (AUBREV.): *IN VITRO*, *IN SILICO* AND *IN VIVO* STUDIES

Sarbani Dey Ray[1,2], Sulagna Dutta[3], Pallav Sengupta[4], Nithar Ranjan Madhu[5], Nirupam Das[1], Supratim Ray[1], Adriana Kolesarova[6,7], and Shubhadeep Roychoudhury*[8]*

Address(es): Prof. Supratim Ray, Department of Pharmaceutical Sciences, Assam University, Silchar 788011, India, email: supratimray75@gmail.com; Dr. Shubhadeep Roychoudhury, Associate Professor, Department of Life Science and Bioinformatics, Assam University, Silchar 788011, India, email: shubhadeep1@gmail.com.
[1] Department of Pharmaceutical Sciences, Assam University, Silchar 788011, India.
[2] Dr. B. C. Roy College of Pharmacy and Allied Health Sciences, Bidhannagar, Durgapur 713206, India.
[3] School of Life Sciences, Manipal Academy of Higher Education (MAHE), Dubai 345050, UAE.
[4] Physiology, Department of Biomedical Sciences, Gulf Medical University, Ajman 4184, UAE.
[5] Department of Zoology, Acharya Prafulla Chandra College, New Barrackpore 700131, India.
[6] Institute of Applied Biology, Faculty of Biotechnology and Food Sciences, Slovak University of Agriculture in Nitra, 94976 Nitra, Slovak Republic.
[7] AgroBioTech Research Centre, Slovak University of Agriculture in Nitra, 94976 Nitra, Slovak Republic.
[8] Department of Life Science and Bioinformatics, Assam University, Silchar 788011, India.

*Corresponding author: supratimray75@gmail.com , shubhadeep1@gmail.com

https://doi.org/10.55251/jmbfs.10564

ARTICLE INFO

Received 8. 9. 2023
Revised 31. 1. 2024
Accepted 31. 1. 2024
Published 1. 4. 2024

Regular article

OPEN ACCESS

ABSTRACT

Inflammatory diseases present a significant burden to global health, often requiring targeted and specific therapeutic agents for effective management. *Ziziphus nummularia* (Aubrev.), a traditional medicinal plant, offers a potential source for these agents. This article aims to explore the anti-inflammatory potential of a novel cyclic alkaloid compound isolated from the root bark of *Ziziphus nummularia*. The cyclic alkaloid compound, [(16-methoxy-10-(3-methyl-butyl)-2-oxa-6, 9, 12-triaza-tricyclo [13.3.1.03, 7] nonadeca-1(18), 13, 15(19), 16-tetraene-8, 11-Dione], exhibited promising anti-inflammatory properties. The potential of this isolated compound (IC) was evaluated *in vitro* by measuring the levels of nitric oxide (NO), prostaglandin-E2 (PGE2), and tumor necrosis factor-alpha (TNF-α). Additionally, Absorption, Distribution, Metabolism, and Excretion (ADME) simulations and molecular docking to the TNF-α receptor were carried out for IC. *In vivo* evaluations of both the IC and its ethanolic extract (EE) were performed using carrageenan-induced paw oedema and arachidonic acid/xylene-induced ear oedema tests. The IC showed a higher inhibition of TNF-α compared to other compounds, reaching a maximum inhibition of 88.00% at a concentration of 50.11 µM. *In silico* analysis revealed that IC formed hydrogen bonds with residues, aspartate at position 45 (ASP 45) and glutamine at position 47 (GLN 47). The IC significantly attenuated oedema induced by carrageenan, xylene, and arachidonic acid. Hence, this compound may offer a potential therapeutic approach for treating inflammation in future clinical applications.

Keywords: Anti-inflammatory agents; Molecular docking; Nitric oxide; Oedema; Prostaglandins; Tumor necrosis factor-alpha, *Ziziphus nummularia*

INTRODUCTION

Inflammation is an intricate physiological process orchestrated by a plethora of molecular mediators that regulate and modulate the immune response of body to tissue injury or pathogens (**Cekici *et al.*, 2000; Qian, 2017; Siegfried *et al.*, 2020**). This immunopathological reaction can be attributed to the overabundance of specific mediators present in macrophages (**Davies and Taylor, 2015; Locati *et al.*, 2020**). Key among these mediators is tumor necrosis factor-alpha (TNF-α), interleukins (IL), nitric oxide (NO), and prostaglandins (PG) (**Montgomery and Bowers, 2012; Vignali and Kuchroo, 2012; Zelova and Hosek, 2013**). Each of these molecules plays a pivotal role in instigating and perpetuating the inflammatory cascade (**Habib and Ali, 2011; Ricciotti and Fitzgerald, 2011; Allerton *et al.*, 2018**). However, when their regulatory mechanisms are compromised, leading to overproduction or prolonged activity, they can foster a range of pathological conditions. From a therapeutic standpoint, targeting and diminishing the activity or concentration of these mediators offers a potential avenue for curbing the exacerbation and progression of inflammation.

The Rhamnaceae family encompasses the species *Ziziphus nummularia* (Aubrev.), commonly known as wild jujube. Indigenous to India's semi-arid and dry regions, this plant has been traditionally employed as an herbal remedy by the native populations for a myriad of health complaints including inflammation, cough, cold, diarrhoea, dysentery, and pain (**Bachaya *et al.*, 2009; Upadhyay *et al.*, 2011; Biswas *et al.*, 2017**). Notably, the anti-inflammatory potential of its leaves, as well as those of related species, has been documented in prior research (**Soliman, 2011; Goyal *et al.*, 2012,2013**). While various molecules have been derived from the plant's leaves and fruits, the root bark remains relatively uncharted territory in the scientific literature. However, it is noteworthy to mention that our group had previously identified a triterpene derivative from the root bark, exhibiting both anticancer and anti-inflammatory activities (**Dey Ray and Dewanjee, 2015; Dey Ray *et al.*, 2015**).

In the arena of drug discovery, the technological advent of *in silico* techniques has revolutionized our understanding of drug-receptor interactions, underpinning rational drug design. Particularly, understanding the mechanistic pathways through which novel drugs manifest anti-inflammatory efficacy is paramount. Within this purview, molecular docking has emerged as a computational technique of significant interest, facilitating insights into potential drug-receptor affinities.

Given this context, the present study embarked on a comprehensive exploration to isolate, elucidate the structure, and discern the anti-inflammatory mechanism of a novel cyclic alkaloid compound (referred to as IC) from the root bark of *Z. nummularia* (Aubrev.). This study was structured in four phases. The maiden phase revolved around the isolation of the new chemical entity and subsequent structural determination. Subsequent *in vitro* analyses ascertained the bioactivity of this isolated compound. In the following phase, an *in silico* approach was employed, probing the interaction dynamics of IC with a key inflammatory mediator, TNF-α. The concluding phase encompassed *in vivo* assessments, evaluating the therapeutic implications of IC in a murine model. Concurrently, the therapeutic potential of the ethanolic extract (EE) was determined and juxtaposed against the bioactivity of IC. Employing an integrative approach combining *in vitro* and *in silico* methods, this study thus aimed to shed light on the complete understanding of the anti-inflammatory mechanism of IC, focusing on its interaction dynamics with TNF-α. This molecular insight complements traditional knowledge and prior discoveries related to the therapeutic potential of *Z. nummularia*. The *in vivo* evaluations,

comparing the therapeutic efficacy of IC to an ethanolic extract, further aimed at advancing the understanding of the pharmacological repertoire of the compound. Thus, in addressing the global health implications of inflammatory diseases, this study investigated the anti-inflammatory properties of a novel cyclic alkaloid compound (referred to as IC) from the root bark of *Z. nummularia*. The comprehensive, multi-pronged approach adopted in this research underscores the meticulous and holistic approach to affirming the therapeutic promise of the compound.

MATERIALS AND METHODS

Plant material

The root barks of *Z. nummularia* (Aubrev.) were collected from Durgapur, West Bengal, India (20º56′ N, 84º53′ E). The plant species was identified and authenticated by the taxonomists from Botanical Survey of India, Shibpur, Howrah, West Bengal [Ref. no.:CNH/I-I/20/2010/Tech.II/171]. A voucher specimen (BCRCP/DP/PT/02/06) has been deposited in the Herbarium of Dr. B. C. Roy College of Pharmacy & Allied Health Sciences, Durgapur, West Bengal, India for future reference.

Extraction, isolation, and identification

2.5 kg of powdered root barks were macerated in 5 litres of 70% (v/v) ethanol for a week (35 ± 5 ºC) with intermittent shaking and stirring. Filters were used to remove particulate matters and cellular debris from the extracts. Finally, crude extract was concentrated in a rotary vacuum evaporator at low heat (< 40 ºC) under reduced pressure to obtain the semi-solid extract (55 g). As a result, the extract yield was 2.2 percent (w/w). The extract was kept in a desiccator. 15.38g crude extract was combined with 32.14g of 60-120 mesh silica gel to make an admixture for isolation. Then a 2.4cm diameter column was packed with 30.05g of 60-120 mesh silica gel and 47.52g of chloroform admixture. The column was then eluted with solvents increasing in polarity (chloroform to methanol). The isolated chemical yielded 0.075g (0.48 percent w/w).
Several fractions undergoing TLC analysis and plates were sprayed with reagents for initial identification of phytoconstituents. HPTLC analysis was done using CAMAG HPTLC. Melting point was measured and uncorrected. ^{1}H NMR, ^{13}C NMR were done using Bruker 400 MHz instrument (Bruker, Germany). IR spectrum was performed with KBr on FTIR-8400S (Shimadzu, Japan). Mass spectrum was done on LC-MS/MS (API- 4000 TM, Applied BioSystems, MDS SCIEX, Canada). The high-resolution mass spectrum was carried out on Thermo-Fisher Orbitrap Exploris 120 Mass Spectrometry (MS) system. Elemental analyses were performed on a Perkin Elmer (2400 Series II) analyzer (Perkin Elmer, USA).

Test materials and chemicals

The EE and IC utilized in the animal experiment were suspended in 1% tween-80 as a solvent. In this study, DMSO was used to solubilize IC in a master plate (resulting less than 0.4 percent DMSO concentration to avoid cytotoxicity in DMSO-producing cells). A variety of concentrated IC solutions in 100 percent DMSO were diluted in master plate. Briefly, a variety of concentrated IC solutions in (100 percent DMSO) were transferred in master plate. The dilution was then finished in a drug dilution plate (1:25 dilution ensuing 4 percent of DMSO). Finally, the cells received the desired concentration of IC solution (1:10 dilution producing 0.4 percent of DMSO).
RAW 264.7 cell line was obtained from SIGMA-RBI, Switzerland. Dulbecco's Modified Eagle Medium (DMEM) both with and without phenol red, phosphate buffered saline (PBS) and Griess reagent was obtained from Invitrogen (Carlsbad, USA). Lipopolysaccharide (LPS), foetal bovine serum (FBS) from *E. coli* serotype 0111: B4, and interferon gamma (IFNγ) were purchased from BD Biosciences (New Jersy, USA). Other reagents and chemicals were of HPLC grade.

In vitro inflammation inhibitory activity

Preparation of cell culture and stimulation

RAW 264.7 murine monocytic macrophage cell line was maintained in DMEM supplemented with 10% FBS, 4.5 g/l glucose, sodium pyruvate (1 mM), L-glutamine (2 mM), streptomycin (50 µg/ml), and penicillin (50 U/ml) at 37 °C in the presence of 5% CO_2. Cells with a confluency of 80–90% were centrifuged at 120g for 10 minutes at 4 °C to obtain a final cell concentration of 2×10^6 cells/ml. 50 µL of cell suspension was placed to a 96-well tissue culture plate (4×10^5 cells/well). Then it was incubated at 37 °C for 2 hours in the presence of 5% carbon dioxide. Following that, 100 U/ml IFN- γ and 5 µg/ml LPS were given to the cells with / without the IC evaluated, with a final volume of 100 µL/well using DMSO as the vehicle. For the next 20 hours, the cells were incubated at 37°C in the presence of 5% carbon dioxide.

Estimation of NO, PGE2, and TNF-α inhibitory activity of IC

NO was estimated by Griess reagent as build-up of nitrite (**Titheradge, 1998**). It was quantified using sodium nitrite as a standard. PGE2 and TNF-α in supernatant were estimated by ELISA kits (eBioscience, USA) as per manufacturer's instructions.

In silico ADME computation and molecular docking studies of IC

The ADME of the IC was calculated using an *in silico* method. Maestro Schrodinger (MS) programme [QikProp® (Version 3.2) module] created a pharmacokinetic outline of IC. At first IC was counterbalanced. Several descriptors including Lipinski's rule were calculated. The conformity of IC to Lipinski's rule indicates potential for the molecule for future development.

Prediction of active site and molecular docking

The inflammation inhibition of IC on TNF-α was considered to explore the exact form of inhibition of selected TNF-α receptor. Maestro 9.0 build panel was used for construction of 3D configurations of IC (Schrödinger, LLC., USA). In this panel LigPrep 2.3 version was employed.

Preparation of the protein and prediction of active site

The protein was recombinant human TNF- α (resolution of 2.30 Å and crystal in nature) and was chosen from an available source (PDB ID: 1A8M) (**Reed *et al.*, 1997**). The Maestro Schrödinger®9.0 module was used to ground the structure as well as anticipate the active site. Because the selected TNF- α receptor lacked a correlated co–crystallized ligand, the exact location of the critical binding region on the receptor was unknown. As a result, the Sitemap® module (Maestro Schrödinger® 9.0, version v23118) was used to locate a promising binding hollow space within the receptor. Two binding sites were found in the output, and the binding site with the highest score (0.643) was chosen for molecular docking.

In vivo anti-inflammatory activity

Animal experiments were performed as per ethical committee's recommendations (Ref No: BCRCP/IAEC/8/2012). Albino mice (♂, 25±5 g, age: 2–3 months, n=6 per group) were kept inside standard polypropylene cages (3 mice/cage) at model laboratory environment of 12:12 light–dark cycle. The temperature as well as relative humidity was 20 ± 2 °C and 55 ± 5 %, respectively.

Acute toxicity study

The study on the acute toxicity of EE and IC were performed according to **Lorke (1983)**. The detailed procedure is given in **Supplementary Figures**.

Carrageenan induced oedema of paw in mice

Carrageenan-induced paw oedema in mice is a useful approach for evaluating the anti-inflammatory potential of active phytoconstituents (**Dordevic *et al.*, 2007**). Mice were starved for 12 hours prior to the experiment. Sixty mice were divided into six groups (n=10). Group 1 received tween-80 (1 %) orally, 30 minutes ahead of carrageenan injection. This group acted as inflammation control. Groups 2 and 3 orally accepted 100 mg/kg and 200 mg/kg EE, respectively. Group 4 as well as 5 orally received 400 µg/kg and 600 µg/kg of IC, respectively. Group 6 was given aspirin (10 mg/kg) and acted as positive control. Following carrageenan administration, paw oedema was measured at 0 hour, 1 hour, 2 hours, 3 hours, 4 hours, and 5 hours.

Xylene/arachidonic acid-produced oedema of ear

For each model, mice were divided into six groups (n=10). Inflammation was generated in mice by applying 30 µl of following reagents: arachidonic acid 0.1 mg/µl in acetone (**Young *et al.*, 1984**) and xylene (**Nunez Guillen *et al.*, 1997**) on inner and outer faces of right ear. Group 1 received tween-80 (1 %) orally, 30 minutes ahead carrageenan injection. This group acted as inflammation control. Groups 2 and 3 orally accepted 100 mg/kg and 200 mg/kg EE, respectively. Groups 4 and 5 orally received 400 µg/kg and 600 µg/kg of IC, respectively. Group 6 was given aspirin (10 mg/kg) and acted as positive control. Left ear acted as normal control. All the mice were sacrificed 30 minutes after arachidonic acid injection/xylene administration. The ears were then taken away and weighed.

Statistical analysis

Results were presented as mean ± standard error of mean (SEM). The impact of the values was checked by student *t* test using computerized GraphPad InStat (version 3.05), GraphPad software, USA. Differences were considered statistically significant at $p<0.05$.

RESULTS

Preliminary structural characteristics of the isolated compound (IC)

The fractions numbered 49 to 56, obtained from column chromatography, displayed a predominant spot with minor impurities when analyzed on thin-layer chromatography (TLC) using silica gel plates. The visualization of these spots was achieved by treating the plates with Dragendorff's reagent. To remove the observed impurities, these fractions were washed with hexane. Following the washing, fractions 49 to 56 were combined and consolidated. A subsequent purification step involved another hexane wash. From this process, a total yield of 0.075 grams of the compound was obtained.

The purified, bioactive eluent was further subjected to high-performance thin-layer chromatography (HPTLC) for detailed analysis. Detection was carried out at a wavelength of 450 nm. The mobile phase used for the chromatography consisted of a solvent system: methanol, ethyl acetate, chloroform, and formic acid in the ratio of 1:7:2:0.2. The retention factor (Rf) value of the compound was found to be 0.59. Additional HPTLC data included a peak height of 2.8 and an area under the peak measuring 111 (**Supplementary Figure 1)**.

The melting point (m.p.) of the purified compound was determined to be in the range of 465-468 °C. An elemental analysis was performed on the isolated compound with the molecular formula $C_{21}H_{29}N_3O_4$. The calculated percentage composition was Carbon (C), 65.09%; Hydrogen (H), 7.54%; Nitrogen (N), 10.84%; and Oxygen (O), 16.52%. The experimental findings from the analysis closely matched the calculated values with percentages: C, 65.17%; H, 7.55%; N, 10.86%; and O, 16.54%.

This approach and the subsequent data helped in the isolation and preliminary structural elucidation of the compound of interest.

The isolated compound showed following spectral characteristics:

^{1}HNMR ($CDCl_3$): δ 4.336 (d, *J*=9.6, H-3), 1.971 (d, *J*=6.4, H-4), 2.803 (s, H-5), 8.516 (d, H-6), 4.632 (d, *J*=14.8, H-7), 8.475 (s, H-9), 4.761 (d, *J*=11.2, H-10), 8.452 (s, H-12), 7.530 (t, *J*=6.0 Hz, H-13), 7.380 (d, *J*=4.4 Hz, H-14), 6.977 (d, *J*=15.2 Hz, H-15), 6.742, (d, J=10.4 HZ, H-17), 6.904 (d, *J*=16.4 Hz, H-18), 7.214 (s, *J*=4.8 Hz, H-19), 3.817 (s, *J*=4.0 Hz, H, of -OC<u>H</u>$_3$), 1.712 (s, H-10-1'), 1.298 (s, *J*=4.0, H-10-2'), 1.987(d, *J*=6.4, H-10-3'), 0.947 (d, *J*=13.6 Hz, H-10-4') **(Supplementary Figures 2 – 5).**

^{13}CNMR ($CDCl_3$): δ 150.240 (-*C*H=, C-1 / 16), 77.017 (*C*H-, C-3), 39.176 (*C*H$_2$-, C-4 / 5), 171.196 (-*C*=O, C-8 / 11), 55.874 (-*C*H-, C-10), 32.432 (*C*H$_2$-, C- 10-1', 10-2'), 29.706 (*C*H- C-10-3'), 14.771(-*C*H$_3$, C-10-4'), 118.17 (*C*H=, C-13 /14), 128.766 (*C*H- C-15), 60.369 (-O*C*H$_3$, O-<u>C</u>H$_3$), 113.674 (*C*H-, C-17 / 18 / 19) **(Supplementary Figure 6).**

IR (KBr) ν_{max} 2955, 2869, 1686, 1648, 3065, 3394, 1221, 1033, 883, 1454, 1376 cm^{-1} **(Supplementary Figure 7)**.

MS (FAB; *m/z*): 387. [M+1] **(Supplementary Figure 8)**.

The orbitrap high-resolution MS showed the mass of isolated compound was 378.4711 **(Supplementary figure 9)**. The structure of IC is given in **Figure 1**. To the best of our knowledge this is the first report of the IC, i.e., [(16-methoxy-10-(3-methyl-butyl)-2-oxa-6, 9, 12-triaza-tricyclo [13.3.1.0$^{3, 7}$] nonadeca-1(18), 13, 15 (19), 16-tetraene-8, 11-dione] from this species.

In vitro study

Dose-dependent inhibition of NO and TNF-α production by IC in LPS/IFN-γ stimulated RAW 264.7 cells

Treatment of cells (RAW 264.7) with LPS/IFN- γ was found to increase the concentrations of NO, TNF- α, and PGE2 (**Figure 2**). The effect of IC on NO production was dose-dependent, with the highest inhibition being 67.00 percent at 50118.72 nM (~50.11 μM). PGE2 inhibition, on the other hand, did not appear to be dose-dependent, with the maximum inhibition of 55.00 percent noted at 100 nM. IC also had a concentration-dependent effect on TNF- α production. The highest inhibition was 88.00 percent at 50.11 μM. IC had the most inhibitory potential on TNF- α production when compared to NO. As a result, TNF- α receptor was used in molecular docking.

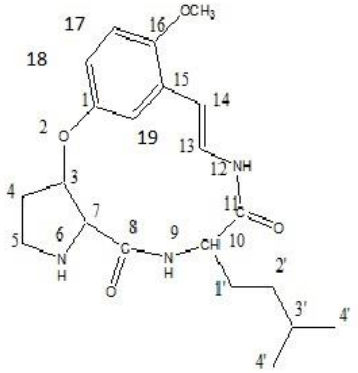

16-Methoxy-10-(3-methyl-butyl)-2-oxa-6,9,12-triaza-tricyclo[13.3.1.0^{3,7}]nonadeca-1(18),13,15(19),16-tetraene-8,11-dione

Figure 1 The structure and chemical name of the isolated compound (IC).

Table 1 Pharmacokinetic prediction of the isolated compound (IC) by QikProp® 3.2.

Sl. No.	Descriptor	Description	Recommended Range	Predicted Value of IC
1	mol_MW	Molecular weight of the molecule	130.0-725.0	387.48
2	SASA	Total solvent accessible surface area (SASA) in square angstroms using a probe with a 1.4 A^0 radius	300.0-1000.0	645.49
3	FOSA	Hydrophobic component of the SASA (saturated carbon and attached hydrogen)	0.0-750.0	456.87
4	FISA	Hydrophilic component of the SASA (SASA on N, O and hydrogen on heteroatom)	7.0-330.0	94.90
5	PISA	Π (carbon and attached hydrogen) component of SASA	0.0-450.0	93.66
6	volume	Total solvent-accessible volume in cubic angstroms using a probe with 1.4 A^0 radius	500.0-2000.0	1203.93
7	donorHB	Estimated number of hydrogen bonds that would be donated by the solute to water molecules in an aqueous solution. Values are averages taken over a number of configurations, so they can be non-integer	0.0-6.0	2.25
8	accptHB	Estimated number of hydrogen bonds that would be accepted by the solute to water molecules in an aqueous solution. Values are averages taken over a number of configurations, so they can be non-integer	2.0-20.0	7.25
9	QPlogP o/w	Predicted octanol / water partition coefficient	-2.0-6.5	1.992
10	Human oral absorption	Predictive qualitative human oral absorption. The assessment uses a knowledge-based set of rules, including checking for suitable values percent human oral absorption, number of metabolites, number of rotatable bonds logP, solubility and cell permeability	1, 2, 3 for low, medium and high absorption respectively	3
11	% human oral absorption	It predicts human oral absorption on 0 to 100% scale. The prediction is based on a quantitative multiple linear regression model. This property usually correlates well with human oral absorption.	>80% is high <25% is poor	80.65
12	#rtvFG	This particular descriptor indicates the number of reactive functional groups. The presence of these groups can lead to decomposition, reactivity, or toxicity problems *in vivo*.	0 to 2.0	0
13	CNS	Predictive central nervous activity on a –2 (inactive) to +2 (active) scale.	-2.0 to 2.0	0
14	Lipinski's rule of five	Lipinski's rules of five are: mol_MW< 500, QPlogPo/w < 5, donorHB ≤ 5, accptHB ≤ 10. Compounds that satisfy these rules are considered drug like. (The "five" refers to the limits, which are multiples of 5).	Maximum is 4	Satisfy the Lipinski's rule of five

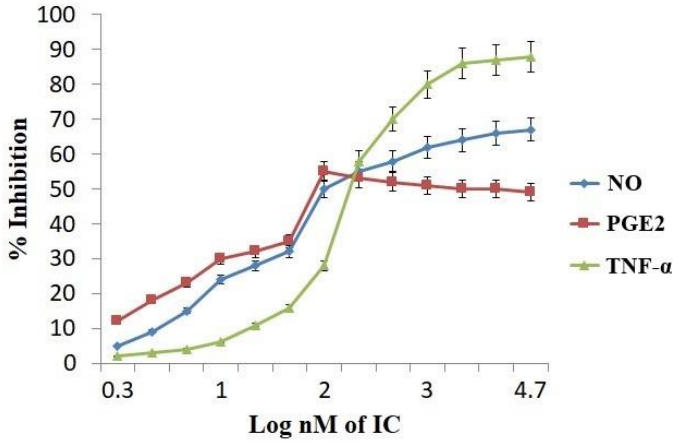

Figure 2 Effect of the isolated compound (IC) on nitric oxide (NO), prostaglandin-E2 (PGE2), and tumor necrosis factor-alpha (TNF-α) production to demonstrate its inflammatory inhibition potential.

***In silico* study**

Physicochemical and ADME computational analysis of IC in relation to its drug-likeness and interaction with TNF-α receptor

The physicochemical properties of the IC were evaluated to ascertain its drug-likeness. Molecular weight (MW), QPlogP (which is a measure of the partition coefficient between octanol and water), the number of hydrogen bond donors (donorHB), and the number of hydrogen bond acceptors (accptHB) were examined with respect to Lipinski's rule of five. The estimated values for these parameters fell within the designated acceptable ranges, indicating that the IC exhibits properties consistent with known drug molecules (**Lipinski *et al.*, 2001**).
Further computational assessments were conducted to gain insights into the physicochemical characteristics of IC. The solvent accessible surface area (SASA) was determined to be 645.49. The hydrophobic and hydrophilic components of SASA, which are denoted as FOSA and FISA respectively, were calculated to be 456.87 and 94.90. Additionally, the π component of the SASA, termed as PISA, was found to be 93.66. The overall volume of the IC was computed to be 1203.93. Such measurements underscore the importance of the solvent-accessible surface area, hydrophobicity, hydrophilicity, and the π component when considering the interaction of IC with TNF-α. Notably, the aforementioned values fit within the stipulated acceptable ranges, suggesting that IC has a propensity to bind along the hydrophilic-hydrophobic interface of the TNF-α receptor.
Parameters concerning oral bioavailability and the presence of reactive functional groups were evaluated. The oral absorption value was computed to be 3, while the percentage of oral absorption for humans was found to be 80.65. In terms of functional groups that may participate in chemical reactions, a value of 0 was derived, implying that IC is unreactive in this regard. Additionally, the assessment revealed that IC is not active within the central nervous system (CNS) (**Table 1**).

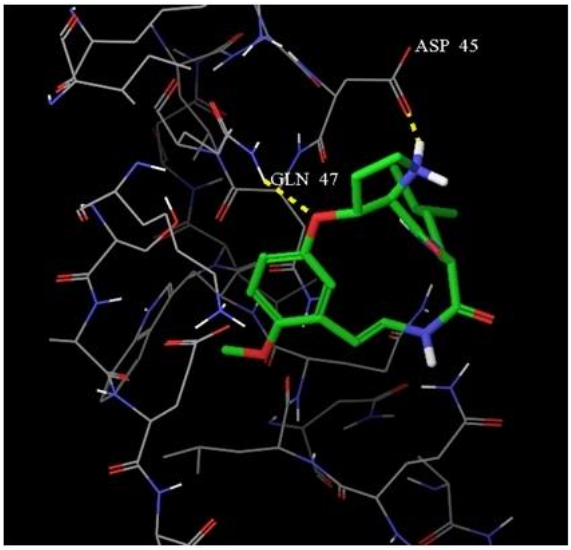

Figure 3 Three-dimensional (3-D) view of docking pose of minimum energy structure complex of the isolated compound (IC) docked at the predicted active site of tumor necrosis factor-alpha (TNF-α) (PDB ID: 1A8M) viewed using Glide XP visualizer of Schrödinger Maestro. Hydrogen bonds are shown as yellow dash and bonded with ASP 45 and GLN 47.

Molecular docking of ligand IC with TNF-α receptor: interaction with residues ASP 45 and GLN 47

In the molecular docking study, the ligand IC established two distinct hydrogen bonds with the amino acid residues of the protein target, TNF-α receptor. Specifically, the residues ASP 45 and GLN 47 were involved in this interaction (**Figure 3**).
The oxygen atom within the linkage of IC functioned as a hydrogen bond acceptor, forming bonds with the side chains of both GLN 47 and ASP 45. In contrast, the –NH group present in the pyrrolidine ring of IC acted as a hydrogen bond donor.

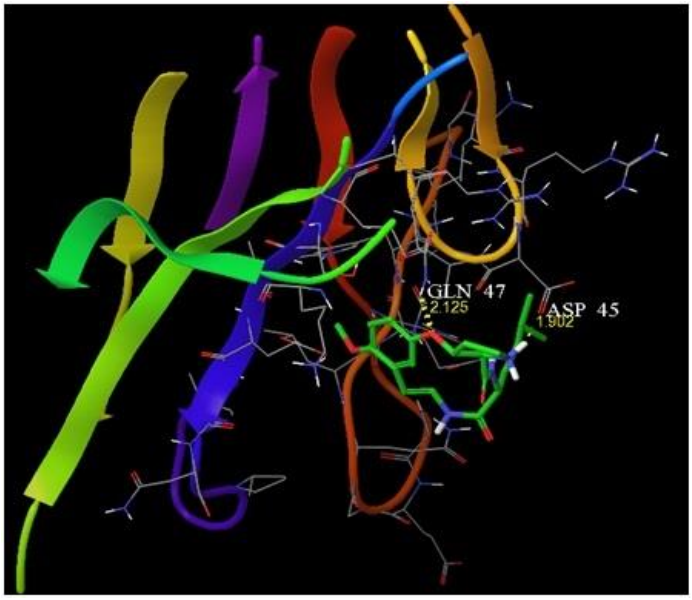

Figure 4 Docked pose of the isolated compound (IC) complemented by the hydrophilic-hydrophobic shape of tumor necrosis factor-alpha (TNF-α) receptor.

Furthermore, the molecular conformation of IC, when docked onto the protein, appeared to align favourably with the hydrophilic and hydrophobic regions of the TNF-α receptor. This compatibility of IC with the microenvironment of the receptor, as well as its binding interactions, resulted in a calculated docking score (G score) of -5.36, indicating the energetics of the interaction. This docked pose and the interaction details can be further visualized in **Figure 4**.
The negative G score suggests a thermodynamically favourable interaction between IC and the TNF-α receptor, indicative of a potential binding affinity and interaction strength.

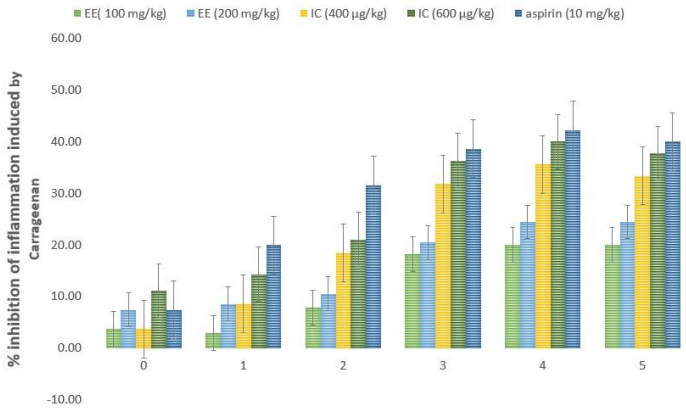

Figure 5 Effect of isolated compound (IC) and ethanolic extract (EE) on carrageenan produced oedema of paw in mice. *p < 0.05 compared with control group.

***In vivo* study**

Acute toxicity study

In male mice, the LD_{50} doses of EE and IC were determined to be 3020 mg/kg body weight (bw) and 2200 mg/kg bw, respectively.

Effect of EE and IC on carrageenan-produced oedema of paw in mice

A well-known and well-established paradigm for acute inflammation is carrageenan-induced inflammation. During the 4th and 5th hours after carrageenan therapy, oral doses of EE at 100 mg/kg and 200 mg/kg were found to reduce inflammation. The percentage inhibitory activities were 20.0 and 24.4, respectively ($p < 0.05$), as compared to control. At the 3rd, 4th, and 5th hours after receiving a 400 µg/kg oral dose of IC, the percentage inhibitions were 31.82, 35.56, and 33.33, respectively ($p < 0.05$). At the same incubation time, percentage inhibitions at 600 µg /kg of IC were 36.36, 40.00, and 37.78, respectively ($p < 0.05$). The percentage inhibitions were 38.64, 42.22, and 40.00 ($p < 0.05$) after the 3rd, 4th, and 5th hours respectively, following aspirin therapy at an oral dosage of 10 mg/kg. The data show that at 4 hours after carrageenan therapy, the percentage inhibition of IC at the aforementioned two doses and aspirin at a dose of 10mg/kg began to decrease. In the case of EE, however, the percentage inhibition remained constant between the 4th and 5th hours (**Figure 5**).

Effect of EE and IC on xylene/arachidonic acid-produced oedema of ear

Inhibition of xylene-induced ear oedema inflammation by EE at 100 mg/kg and 200 mg/kg was 19.51 and 31.71 percent ($p < 0.05$), respectively. For the arachidonic acid-induced model, the inhibitions were 27.06 and 30.59 percent, respectively ($p < 0.05$). The suppression of xylene-induced ear oedema inflammation by IC at 400 and 600 µg/kg was 50.00 and 53.66 percent, respectively ($p < 0.05$). The inhibitions were 48.24% and 52.944% for the arachidonic acid model, respectively ($p < 0.05$). The inhibitions of both models were 57.32 and 61.18 percent, respectively ($p < 0.05$), for aspirin at a dosage of 10 mg/kg (**Figure 6**).

DISCUSSION

The primary objective of this study was to isolate and characterize an active compound from the bark of *Z. nummularia* (Aubrev.), to determine its molecular structure, and to explore its mechanism of action using *in vitro*, *in silico*, and *in vivo* methods. The isolated compound, denoted as IC, is [(16-methoxy-10-(3-methylbutyl)-2-oxa-6, 9, 12-triaza-tricyclo [13.3.1.03, 7] nonadeca-1(18), 13, 15(19), 16-tetraene-8, 11-Dione]. To the best of our knowledge, this study marks the first documentation of its bioactivity.

NO and PGE2 are prominent mediators synthesized by macrophages (**Lin *et al.*, 2014; Shi *et al.*, 2014**). Previous literature suggests that TNF-α acts as an endogenous mediator in LPS-induced shock (**Parameswaran and Patial, 2010; Ye *et al.*, 2016**). The inflammation process is exacerbated by the overproduction of NO, PGE2, and TNF-α, leading to the damage of neighbouring cells and tissues. Consequently, molecules that can attenuate the levels of these inflammatory mediators are prospective candidates for anti-inflammatory agents.

Molecular docking studies provided a simulated environment to evaluate the interaction between IC and the TNF-α-receptor. Amino acid residues involved in this interaction included LYS 90, ASP 45, GLN 27, ARG 131, GLU 23, GLY 24, GLN 47, GLU 135, GLN 25, LEU 26, and ASN 46 (**Figure 7**).

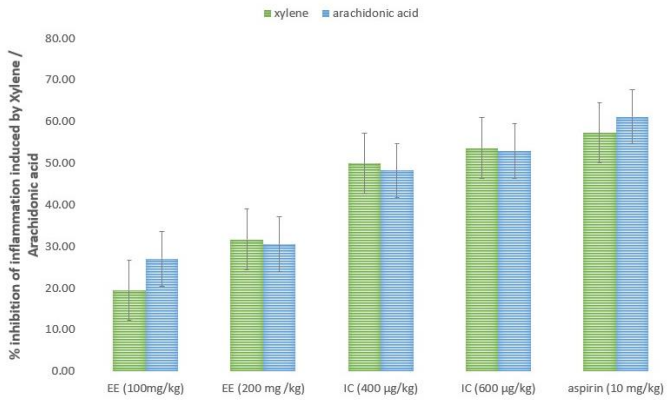

Figure 6 Effect of the isolated compound (IC) and ethanolic extract (EE) on xylene/arachidonic acid-produced oedema of ear. *$p < 0.05$ compared with control group.

Having established the anti-inflammatory potential of IC *in vitro* and supported this finding with *in silico* data elucidating its interaction with TNF-α, the present study proceeded to validate its efficacy *in vivo*. The study employed a carrageenan-induced inflammation model and another model using a combination of xylene and arachidonic acid. The carrageenan test, known for its sensitivity, induces a two-phase oedema in mice due to the surge of inflammatory mediators like NO. The results indicate that IC exhibited a notable inhibitory effect, particularly up to the fourth hour post carrageenan administration. The oedema peak during the third phase of carrageenan-induced inflammation can be attributed to the release of prostaglandins and inherently slow reactions. Additionally, arachidonic acid regulates NO production and serves as a precursor to PGE2, suggesting the observed anti-inflammatory action of IC might stem from the suppression of PGE2 and/or NO synthesis. In the presence of xylene, the release of pro-inflammatory mediators from sensory neurons, mast cells, and other immune cells is facilitated (**Figure 8**).

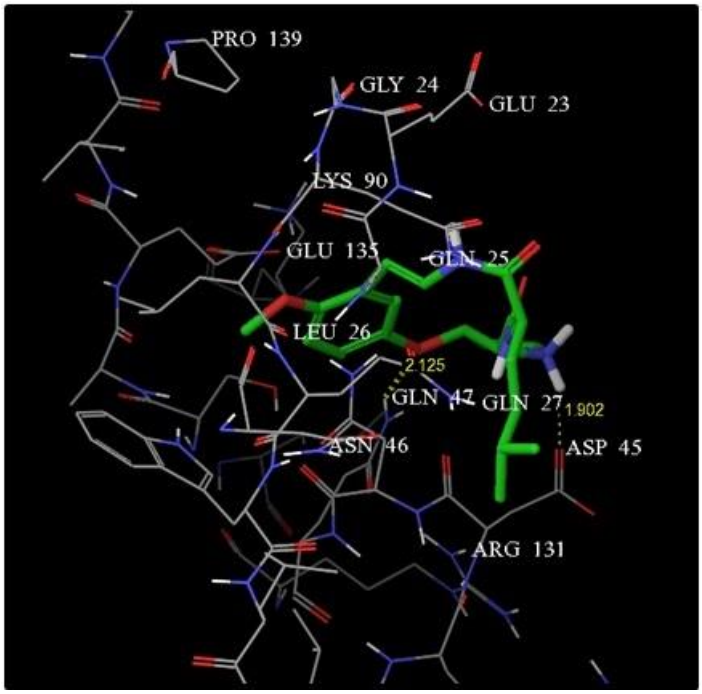

Figure 7 The key amino acid shown within the active site of TNF-α comprising LYS 90, ASP 45, GLN 27, ARG 131, GLU 23, GLY 24, GLN 47, GLU 135, GLN 25, LEU 26, and ASN 46.

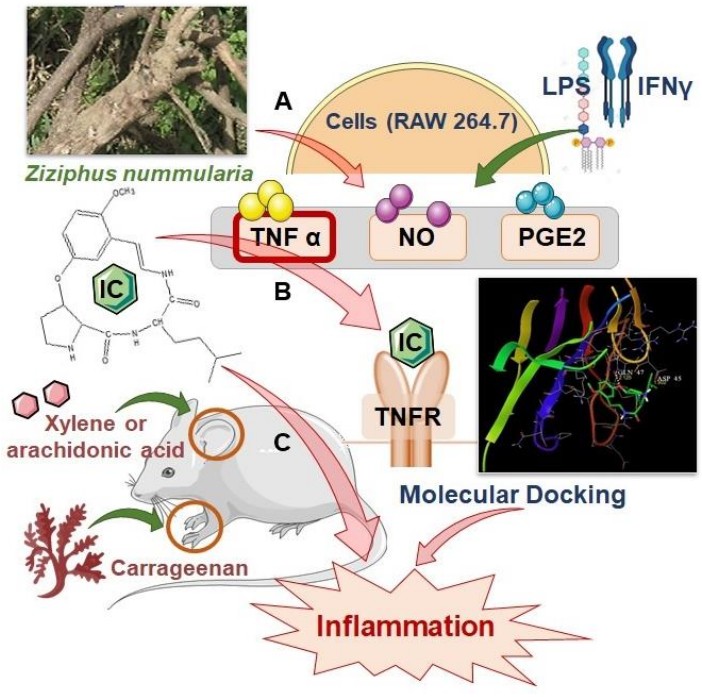

Figure 8 Efficacy of IC as an anti-inflammatory compound, both in cell cultures and animal models, possibly by interacting with the TNF-α receptor and inhibiting the production or effects of specific inflammatory mediators. (A) The anti-inflammatory efficacy of IC shown *in vitro* on RAW 264.7 cells when treated with lipopolysaccharide/interferon-gamma (LPS/IFN-γ). LPS/IFN-γ treatment leads to an increase in nitric oxide (NO), tumour necrosis factor-alpha (TNF-α), and prostaglandin E2 (PGE2) in cells. IC demonstrates an ability to inhibit NO and PGE2 production. IC has been observed to inhibit TNF-α production dose-dependently and most profoundly. As a consequence of these observations, molecular docking experiments were initiated with the TNF-α receptor; (B) *In silico* data concerning the interaction between IC and the TNF-α receptor indicates that IC has potential binding affinity with the TNF-α receptor thereby inhibiting its functions; (C) Validating anti-inflammatory potential of IC *in vivo*, two distinct

inflammation mice models were employed: the first incorporated carrageenan-induced pa oedema, and the latter integrated both xylene- and arachidonic acid-induced ear oedema. Thus, IC is a promising anti-inflammatory compound, showcasing efficacy both in cell-based assays and animal models. This potential can possibly be attributed to the interaction of IC with the TNF-α receptor and its ability to curtail the production or effects of specific inflammatory mediators.

CONCLUSIONS

The compound IC, a novel cyclic alkaloid extracted from the bark of *Z. nummularia* (Aubrev.), demonstrated significant anti-inflammatory properties. Our findings reveal that IC effectively mitigated the expression of inflammatory mediators like NO and TNF-α and exhibited a pronounced reduction in carrageenan, xylene, and arachidonic acid-induced oedema. This compound shows promising potential as a therapeutic agent for inflammation management in future clinical applications. The comprehensive, multi-pronged approach adopted in this research evaluates the *in vitro* anti-inflammatory effects of the compound by measuring key inflammatory markers. Additionally, *in silico* pharmacokinetic analyses and interaction studies are conducted, complemented by thorough *in vivo* evaluations. This comprehensive approach emphasizes a rigorous scientific evaluation of the therapeutic potential of the compound, bridging traditional knowledge with contemporary scientific methodologies.

Declaration of interest: The authors declare no conflict of interest.

Acknowledgements: The authors wish to thank Prof. Achintya Saha of Division of Pharmaceuticals & Fine chemicals, Department of Chemical Technology, University of Calcutta for providing computational support to carry out the *in silico* experiment. One of the authors (SDR) also wishes to acknowledge the authority of Dr B C Roy College of Pharmacy & A.H.S for providing the necessary facility for carrying out the animal experiment.

REFERENCES

Allerton TD, Proctor DN, Stephens JM, Dugas TR, Spielmann G, Irving BA. L-Citrulline Supplementation: Impact on Cardiometabolic Health. *Nutrients. 2018; 10(7):* 921-4. https://doi.org/10.3390/nu10070921

Bachaya HA, Iqbal Z, Khan MN, Sindhu ZU, Jabbar A. Anthelmintic activity of Ziziphus nummularia (bark) and Acacia nilotica (fruit) against Trichostrongylid nematodes of sheep. J Ethnopharmacol. 2009; 123(2): 325-9. https://doi.org/10.1016/j.jep.2009.02.043

Biswas S, Shaw R, Bala S, Mazumdar A. Inventorization of some ayurvedic plants and their ethnomedicinal use in Kakrajhore forest area of West Bengal. J Ethnopharmacol. 2017; 197: 231-41. https://doi.org/10.1016/j.jep.2016.08.014

Cekici A, Kantarci A, Hasturk H, Van Dyke TE. Inflammatory and immune pathways in the pathogenesis of periodontal disease. Periodontol. 2000; 64 (1):57-80. https://doi.org/ 10.1111/prd.12002

Davies LC, Taylor PR. Tissue-resident macrophages: then and now. Immunology. 2015; 144 (4): 541-8. https://doi.org/10.1111/imm.12451

Dey Ray S, Dewanjee S. Isolation of a new triterpene derivative and in vitro and in vivo anticancer activity of ethanolic extract from root bark of *Zizyphus nummularia* Aubrev. Nat Prod Res. 2015; 29(16): 1529-36. https://doi.org/10.1080/14786419.2014.983921

Dey Ray S, Ray S, Zia-Ul-Haq M, De Feo V, Dewanjee S. Pharmacological basis of the use of the root bark of *Zizyphus nummularia* Aubrev. (Rhamnaceae) as anti-inflammatory agent. BMC Complement Altern Med. 2015; 15: 416. https://doi.org/10.1186/s12906-015-0942-7

Dordevic S, Petrovic S, Dobric S, Milenkovic M, Vucicevic D, Zizic S, Kukic J. Antimicrobial, anti-inflammatory, anti-ulcer and antioxidant activities of Carlina acanthifolia root essential oil. J Ethnopharmacol. 2007; 109(3): 458–63. https://doi.org/10.1016/j.jep.2006.08.021

Goyal M, Ghosh M, Nagori BP, Sasmal D. Analgesic and anti-inflammatory studies of cyclopeptide alkaloid fraction of leaves of *Ziziyphus nummularia*. Saudi J Biol Sci. 2013; 20 (4): 365–71. https://doi.org/10.1016/j.sjbs.2013.04.003

Goyal M, Sasmal D, Nagori BP. Analgesic and anti-inflammatory activity of ethanolic extract of *Zizyphus nummularia*. Res J Med Plant. 2012; 6: 521-8. https://doi.org/10.3923/rjmp.2012.521.528

Habib S, Ali A. Biochemistry of nitric oxide. Indian J Clin Biochem. 2011; 26(1): 3-17. https://doi.org/10.1007/s12291-011-0108-4

Lin CY, Lee CH, Chang YW, Wang HM, Chen CY, Chen YH. Pheophytin a inhibits inflammation via suppression of LPS-induced nitric oxide synthase-2, prostaglandin E2, and interleukin-1β of macrophages. Int J Mol Sci. 2014; 15(12):22819-34. https://doi.org/ 10.3390/ijms151222819

Lipinski CA, Lombardo F, Dominy BW, Feeney PJ. Experimental and computational approaches to estimate solubility and permeability in drug discovery and development settings. Adv Drug Deliv Rev. 2001; 46(1-3): 3-26. https://doi.org/10.1016/s0169-409x(00)00129-0

Locati M, Curtale G, Mantovani A. Diversity, Mechanisms, and Significance of Macrophage Plasticity. Annu Rev Pathol. 2020; 15: 123-47. https://doi.org/10.1146/annurev-pathmechdis-012418-012718

Lorke DA. A new approach to practical acute toxicity testing. Arch Toxicol. 1983; 54(4): 275-87. https://doi.org/ 10.1007/BF01234480

Montgomery SL, Bowers WJ. Tumor necrosis factor-alpha and the roles it plays in homeostatic and degenerative processes within the central nervous system. J Neuroimmune Pharmacol. 2012; 7(1): 42–59. https://doi.org/10.1007/s11481-011-9287-2

Nunez Guillen ME, Emim JA, Souccar C, Lapa AJ. Analgesic and anti-inflammatory activities of the aqueous extract of *Plantago major* L. Int J Pharmacogn. 1997; 35(2): 99–104. https://doi.org/10.1076/phbi.35.2.99.13288

Parameswaran N, Patial S. Tumor necrosis factor-α signaling in macrophages. Crit Rev Eukaryot Gene Expr. 2010; 20(2):87-103. https://doi.org/10.1615/critreveukargeneexpr.v20.i2.10

Reed C, Fu ZQ, Wu J, Xue YN, Harrison RW, Chen MJ, Weber IT. Crystal structure of TNF-alpha mutant R31D with greater affinity for receptor R1 compared with R2. Protein Eng. 1997; 10(10): 1101-7. https://doi.org/10.1093/protein/10.10.1101

Ricciotti E, Fitzgerald GA. Prostaglandins and inflammation. Arterioscler Thromb Vasc Biol. 2011; 31(5): 986-1000. https://doi.org/10.1161/ATVBAHA.110.207449

Shi Q, Cao J, Fang L, Zhao H, Liu Z, Ran J, Zheng X, Li X, Zhou Y, Ge D, Zhang H, Wang L, Ran Y, Fu J. Geniposide suppresses LPS-induced nitric oxide, PGE2 and inflammatory cytokine by downregulating NF-κB, MAPK and AP-1 signaling pathways in macrophages. Int Immunopharmacol. 2014; 20(2):298-306. https://doi.org/ 10.1016/j.intimp.2014.04.004

Siegfried G, Descarpentrie J, Evrard S, Khatib AM. Proprotein convertases: Key players in inflammation-related malignancies and metastasis. Cancer Lett. 2020; 473:50-61. https://doi.org/10.1016/j.canlet.2019.12.027

Soliman YH. Topical Anti-inflammatory and wound healing activities of herbal gel of *Ziziphus nummularia* L. (F. *Rhamnaceae*) leaf extract. Int J Pharmacol. 2011; 7(8): 862-7. https://doi.org/10.3923/ijp.2011.862.867

Titheradge MA. The enzymatic measurement of nitrate and nitrite. Methods Mol Biol. 1998; 100: 83–91. https://doi.org/10.1385/1-59259-749-1:83

Upadhyay B, Singh KP, Kumar A. Ethno-veterinary uses and informants consensus factor of medicinal plants of Sariska region, Rajasthan, India. J Ethnopharmacol. 2011; 133(1): 14-25. https://doi.org/10.1016/j.jep.2010.08.054

Vignali DA, Kuchroo VK. IL-12 family cytokines: immunological playmakers. Nat Immun. 2012; 13(8):722–8. https://doi.org/10.1038/ni.2366

Ye H, Wang Y, Jenson AB, Yan J. Identification of inflammatory factor TNFα inhibitor from medicinal herbs. Exp Mol Pathol. 2016; 100(2):307-11. https://doi.org/ 10.1016/j.yexmp.2015.12.014

Young JM, Spires DA, Bedord CJ, Wagner B, Ballaron SJ, De Young LM. The mouse ear inflammatory response to topical arachidonic acid. J Invest Dermatol. 1984; 82 (4): 367–71. https://doi.org/10.1111/1523-1747.ep12260709

Zelova H, Hosek J. TNF- α signalling and inflammation: interactions between old acquaintances. Inflamm Res. 2013; 62 (7): 641–51. https://doi.org/10.1007/s00011-013-0633-0

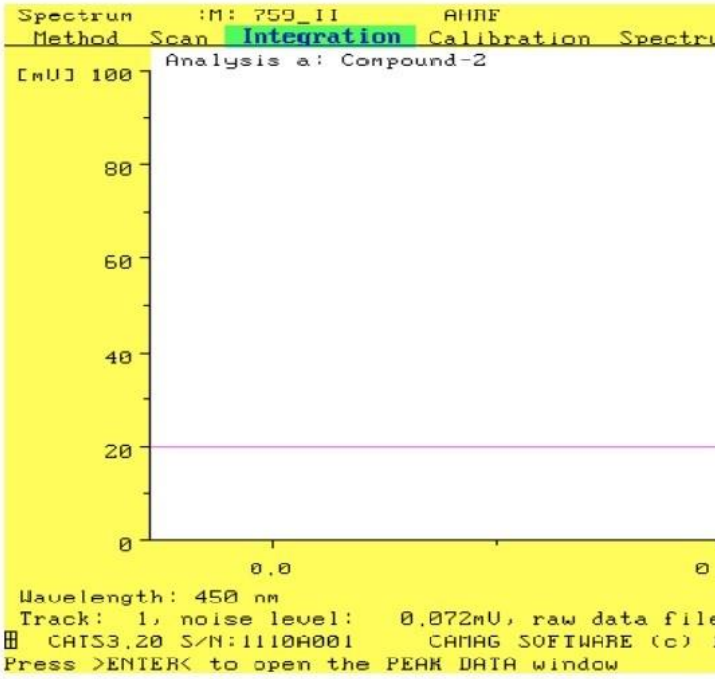

Result table

S. No	Rf	Height	Ar
1	0.59	2.8	11

Supplementary Figure 1 High-performance thin-layer chromatography (HPTLC) profiling of the isolated compound (IC).

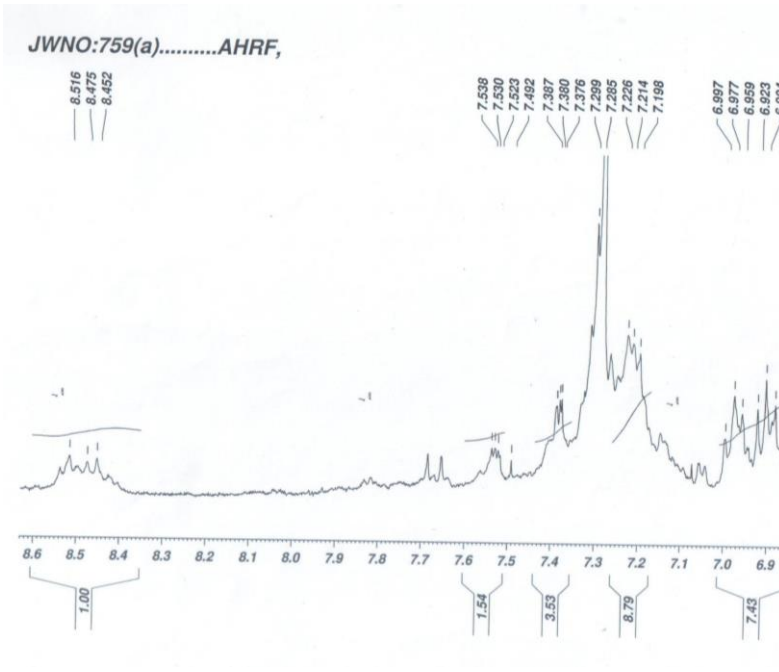

Supplementary Figure 2 ^{1}H nuclear magnetic resonance (^{1}H NMR) spectroscopy of the isolated compound (IC).

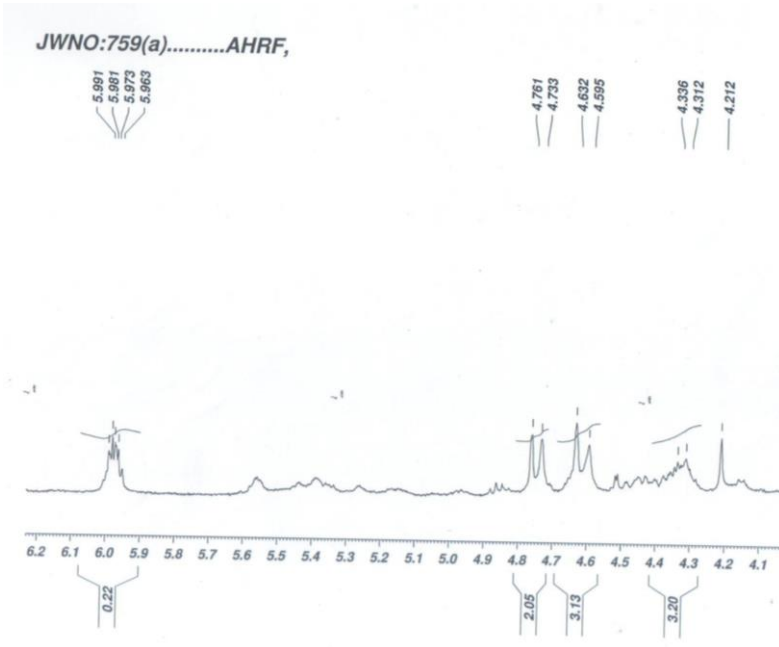

Supplementary Figure 3: ^{1}H nuclear magnetic resonance (^{1}H NMR) spectroscopy of the isolated compound (IC).

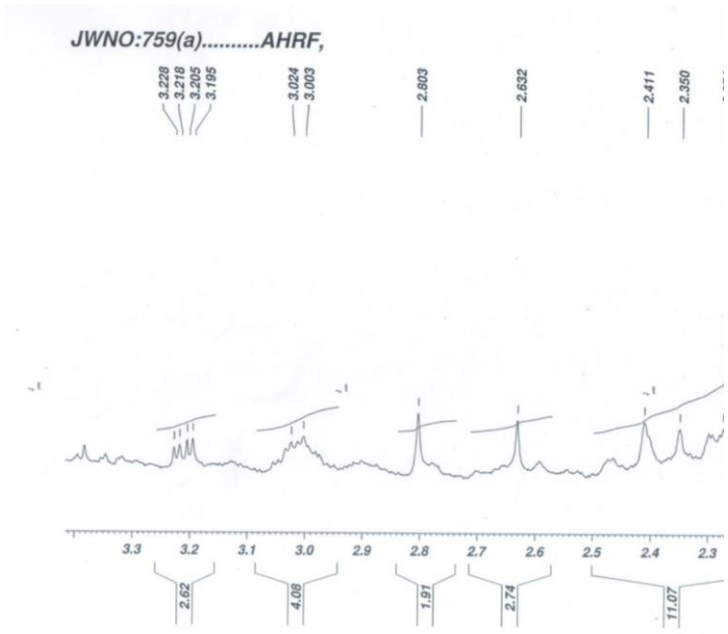

Supplementary Figure 4: ^{1}H nuclear magnetic resonance (^{1}H NMR) spectroscopy of the isolated compound (IC).

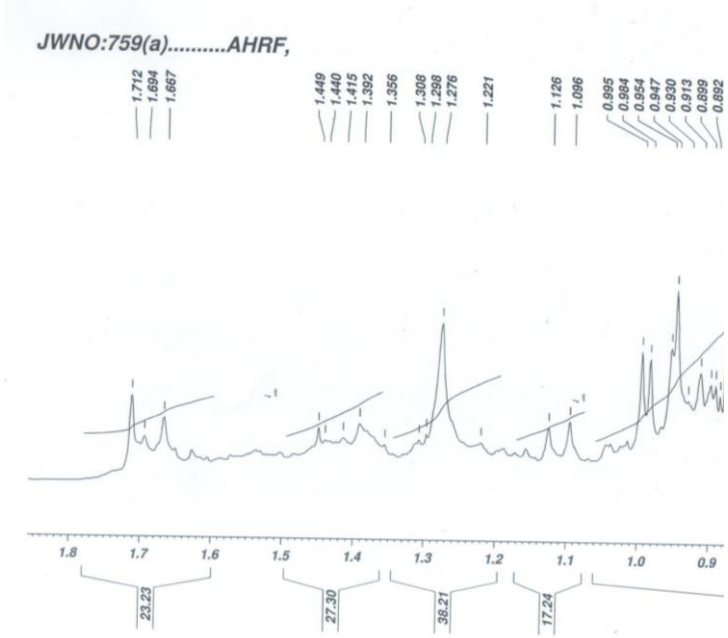

Supplementary Figure 5 ^{1}H nuclear magnetic resonance (^{1}H NMR) spectroscopy of the isolated compound (IC).

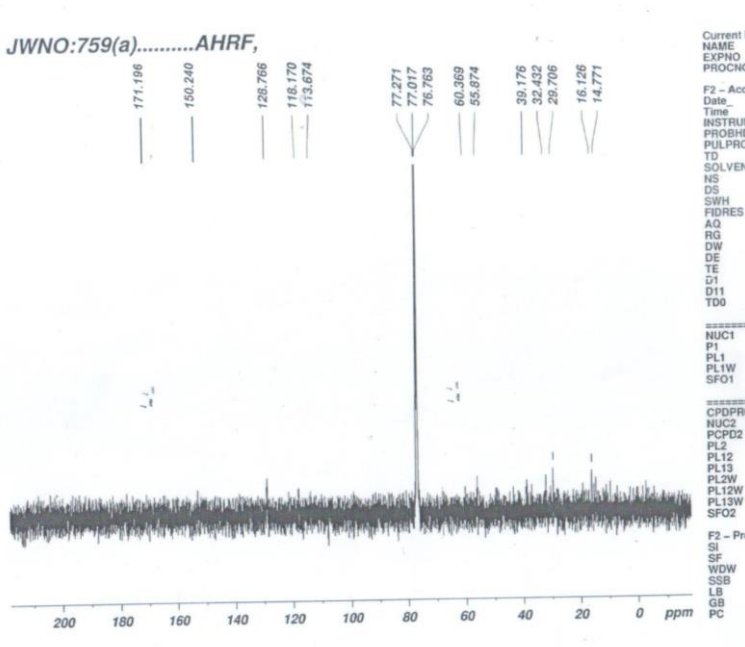

Supplementary Figure 6 ^{13}C nuclear magnetic resonance (^{13}C NMR) of the isolated compound (IC).

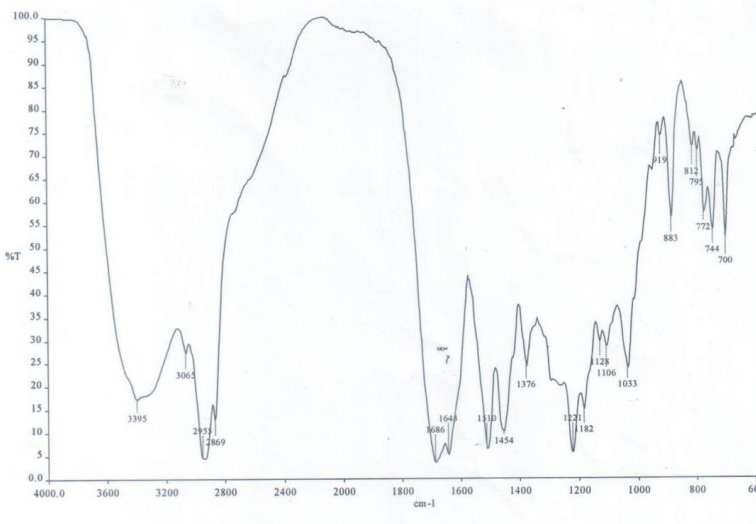

Supplementary Figure 7 Fourier-transform infrared spectroscopy (FTIR) spectroscopy of the isolated compound (IC).

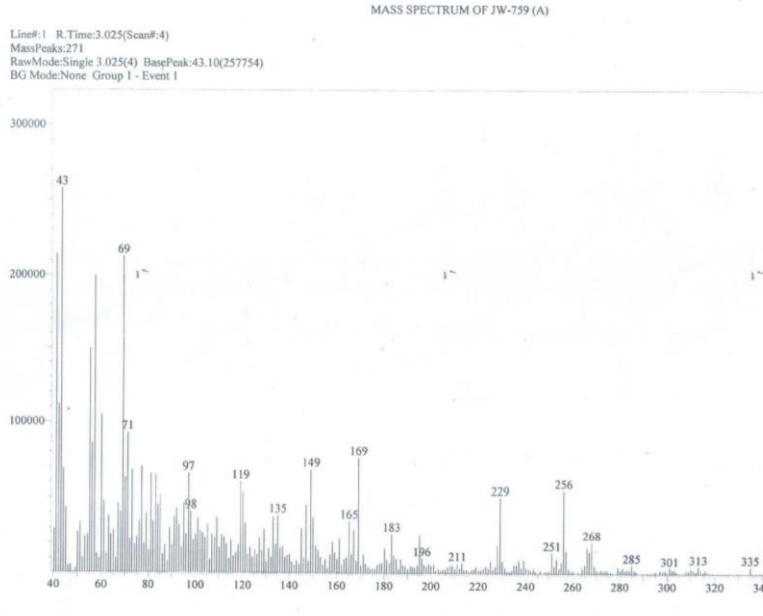

Supplementary Figure 8 Mass spectroscopy of the isolated compound (IC).

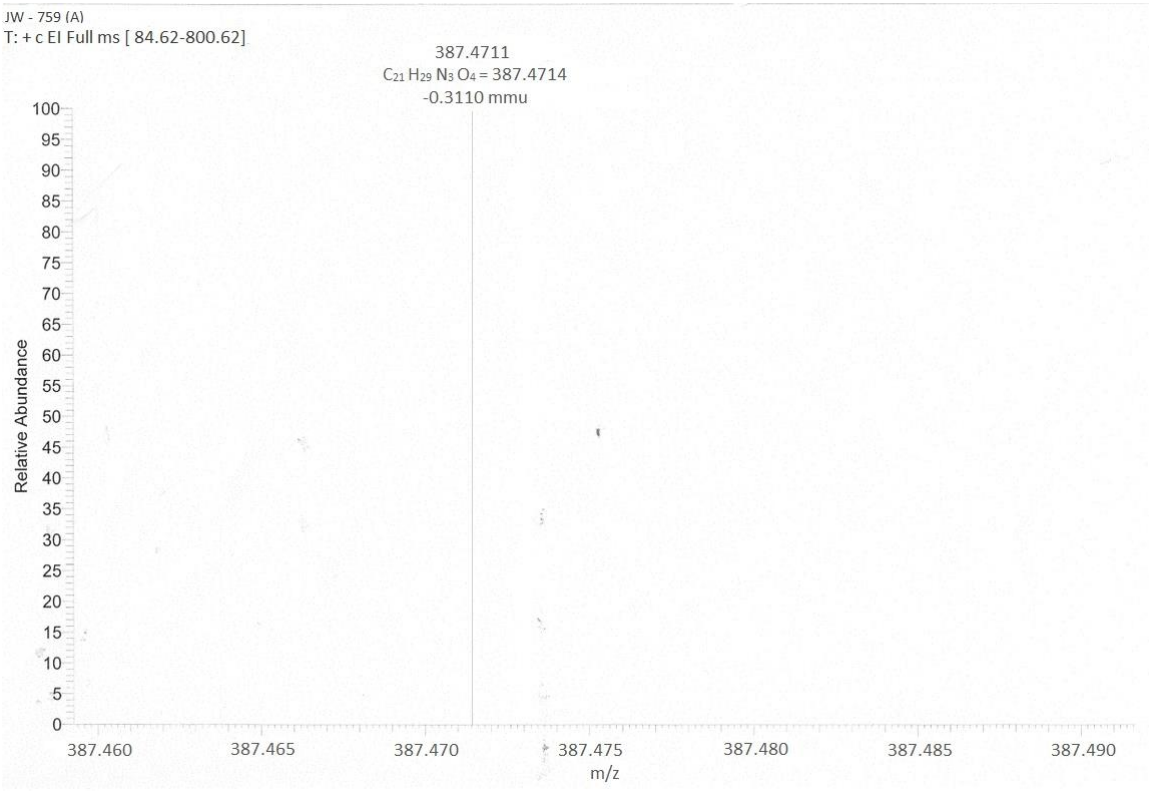

Supplementary Figure 9 High resolution mass spectroscopy of the isolated compound (IC).